



TITLE:

Direct and stepwise energy transfer from excitons to plasmons in close-packed metal and semiconductor nanoparticle monolayer films

AUTHOR(S):

Hosoki, Koshin; Tayagaki, Takeshi; Yamamoto, Shinpei; Matsuda, Kazunari; Kanemitsu, Yoshihiko

CITATION:

Hosoki, Koshin ...[et al]. Direct and stepwise energy transfer from excitons to plasmons in close-packed metal and semiconductor nanoparticle monolayer films. Physical Review Letters 2008, 100(20): 207404.

ISSUE DATE:

2008-05

URL:

<http://hdl.handle.net/2433/87346>

RIGHT:

c 2008 The American Physical Society

Direct and Stepwise Energy Transfer from Excitons to Plasmons in Close-Packed Metal and Semiconductor Nanoparticle Monolayer Films

Koshin Hosoki,¹ Takeshi Tayagaki,¹ Shinpei Yamamoto,¹ Kazunari Matsuda,¹ and Yoshihiko Kanemitsu^{1,2,*}

¹*Institute for Chemical Research, Kyoto University, Uji, Kyoto 611-0011, Japan*

²*Photonics and Electronics Science and Engineering Center, Kyoto University, Kyoto 615-8510, Japan*

(Received 16 January 2008; published 23 May 2008)

We studied the dynamics of photoluminescence (PL) and energy transfer in close-packed monolayer films of CdSe and Au nanoparticles (NPs) assembled using the Langmuir-Blodgett technique. The PL intensity and dynamics depended on the ratio of CdSe to Au NPs in the mixed films. The PL quenching of CdSe NPs occurs through rapid energy transfer from excitons in CdSe NPs to plasmons in Au NPs. The PL decay curves of the mixed NPs monolayers are determined by three decay rates: the direct energy transfer between the nearest-neighbor CdSe and Au NPs (CdSe \rightarrow Au), the stepwise energy transfer from CdSe to CdSe to Au NPs (CdSe \rightarrow CdSe \rightarrow Au), and the radiative recombination in CdSe NPs.

DOI: [10.1103/PhysRevLett.100.207404](https://doi.org/10.1103/PhysRevLett.100.207404)

PACS numbers: 78.67.Bf, 73.21.La, 78.55.Qr

Over the past two decades, semiconductor nanoparticles (NPs) have been studied extensively both experimentally and theoretically because their optical properties can be tuned by changing the size of the NPs and they have potential for optoelectronic applications such as lasers, light-emitting diodes, and solar cells [1–6]. Semiconductor NPs also serve as nanoscale building blocks for tailored materials with fascinating multifunctional properties beyond those of bulk crystals and isolated NPs. Recently, macroscopically ordered NP suprasolids and close-packed NP solids have been prepared, allowing the study of quantum and cooperative phenomena [7,8]. One of the central issues in ordered or close-packed NP solids is the understanding of energy and charge transfer processes on a nanoscale [9].

The optical properties of close-packed NP solids are determined by the electronic interactions between proximal NPs. The electronic interactions between colloidal semiconductor NPs are determined mainly by incoherent long-range dipole interactions [10–12]. Close-packed NP solids have great potential to control the energy flow on a nanoscale [13,14]. In addition, the optical properties of semiconductor NPs change drastically when they contact metal nanostructures [15–18]. The understanding and control of the exciton-plasmon interaction in semiconductor-metal complexes are still an open problem. We anticipate that close-packed mixed solids composed of semiconductor NPs and metal NPs will make it possible to realize novel optical properties. Moreover, they serve as model materials for understanding the microscopic mechanism of the interaction between excitons and plasmons.

In this Letter, we fabricated close-packed monolayer films composed of CdSe and Au NPs using the Langmuir-Blodgett (LB) technique and studied their photoluminescence (PL) dynamics. Time-resolved PL spectroscopy clarified that the PL quenching of CdSe NPs occurs through rapid energy transfer from excitons in CdSe NPs to plasmons in Au NPs. The PL decay curves

of mixed NPs monolayers are described by three exponential decays: the direct energy transfer from CdSe NPs to the nearest-neighbor Au NPs (CdSe \rightarrow Au), the stepwise energy transfer from a CdSe NP to another CdSe NP and then to an Au NP (CdSe \rightarrow CdSe \rightarrow Au), and radiative recombination in CdSe NPs.

As semiconductor NPs, 6.0-nm CdSe/ZnS core-shell NPs (Evident Technologies) were used. Metal Au NPs measuring 8.0 nm were prepared following the procedure in Ref. [19]. The CdSe and Au NPs were mixed in chloroform. Solutions of both were dropped on the fluid surface, and close-packed monolayer films composed of CdSe and Au NPs were fabricated on quartz substrates using the LB technique. The ratios of Au to CdSe NPs in the films were confirmed directly by transmission electron microscopy (TEM).

Figure 1 shows negative tone TEM images of the samples with Au to CdSe NP ratios (Au:CdSe) in the mixed films of (a) 33:67, (b) 72:28, and (c) 100:0. To count the number of the NPs, we used negative tone images. The numbers of Au (N_{Au}) and CdSe (N_{CdSe}) NPs were measured directly by counting in two different $500 \times 500\text{-nm}^2$ areas in each sample. Here, the fraction of Au NPs is defined as $x = N_{\text{Au}}/(N_{\text{Au}} + N_{\text{CdSe}})$. The NPs form a dense, close-packed monolayer with a simple two-dimensional hexagonal lattice. Well-mixed samples with no aggregation of Au and CdSe NP regions were used for optical measurements.

Figure 2(a) shows the absorption spectra of CdSe/Au NP monolayers with various fractions x . In the pure CdSe NP film ($x = 0$), an absorption peak appears around 2.05 eV, and is assigned to the lowest-energy $1S-1S$ exciton state [1,6]. With increasing x , a broad absorption band appears near 2.35 eV, attributable to the surface-plasmon resonance of the Au NPs. The peak gradually shifts to 2.0 eV in the pure Au NP film ($x = 1$). This shift is due to the increase in the background dielectric constant

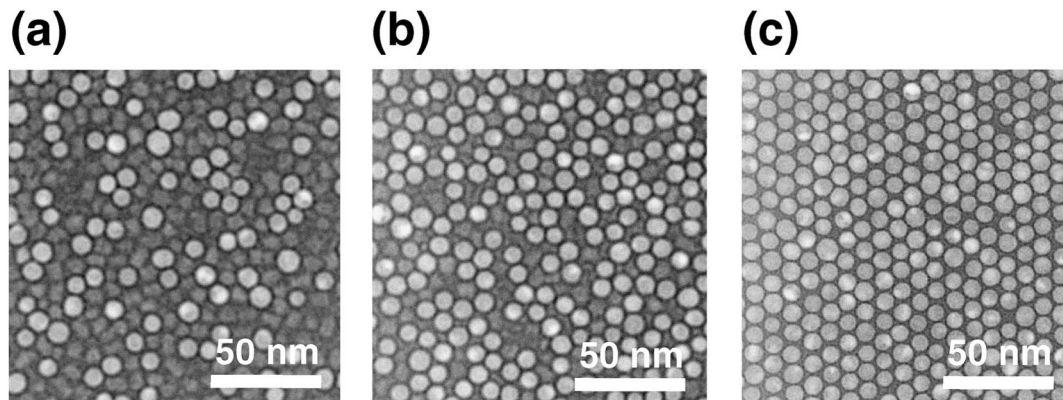


FIG. 1. Typical negative tone TEM images of close-packed Au/CdSe NP mixed monolayer films. Au NPs appear as whitish dots, while CdSe NPs appear as gray dots. The averaged NP ratio (Au:CdSe) of the film is (a) 33:67, (b) 72:28, and (c) 100:0.

around Au NPs with the Au NP ratio [20]. These absorption spectra also support the formation of homogeneous monolayer films.

The inset of Fig. 2(b) shows PL spectra under continuous wave (cw) 3.06 eV laser excitation. As x increases, the PL intensity decreases, although the spectral shapes do not change. The origin of the PL band is assigned to the transition from the lowest exciton state in CdSe NPs in the mixed films. Figure 2(b) shows the PL intensity as a function of x in the mixed film. The normalized PL intensity decreases rapidly as the Au NP ratio increases. Because in the case of no interaction between the NPs the PL intensity is proportional to the number of CdSe NPs in the sample, we draw the ratio of the CdSe NPs in the film as the broken line. The difference between the experimental results and the broken line suggests the existence of the electronic interaction between the CdSe and Au NPs. On doping CdSe NP solids with Au NPs, PL quenching occurs through the interaction between CdSe and Au NPs.

To further quantify the interaction between CdSe and Au NPs, we measured time-resolved PL spectra in each

sample under 3.1 eV and 150 fs laser excitation using a streak camera. The PL dynamics in CdSe NPs dispersed in chloroform were also measured under the same experimental conditions. In the nanosecond time region, spectrally resolved PL decay curves of isolated CdSe NPs in solutions were described by a single exponential function with a time constant of about 12 ns at 2.0 eV. No clear rapid decay components due to multiexcitons and Auger recombination were observed [6,21]. Under our experimental conditions, we confirmed that the PL decay dynamics are independent of the excitation intensity and many body effects of excitons in CdSe NPs do not play an essential role in the PL decay dynamics in close-packed films.

Figure 3 shows the temporal change in the PL intensity near 2.0 eV, in each monolayer sample. In the close-packed CdSe NPs monolayer samples ($x = 0$), the PL decay curves can be approximated by two exponential functions. Note that a fast decay component of about 1 ns appears in close-packed monolayer films, but not in isolated NP solutions. This observed value is close to the value reported for CdSe films [11,12]. Our results imply that the 1-ns

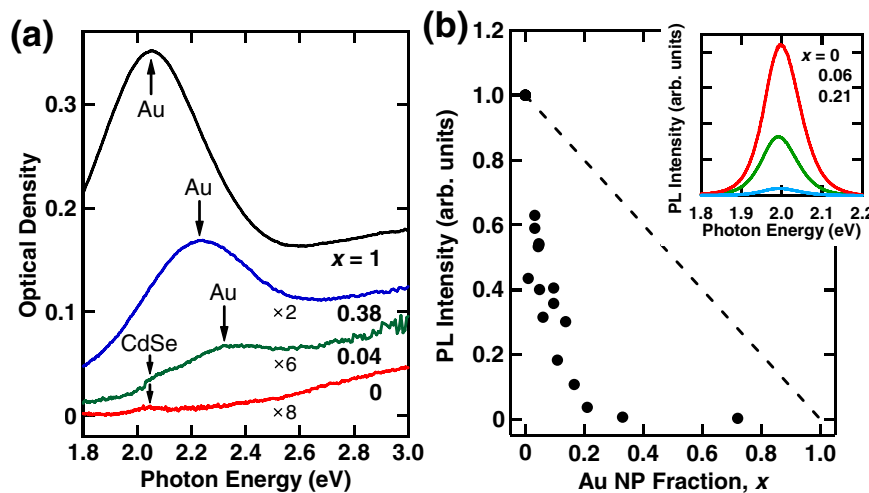


FIG. 2 (color online). (a) Absorption spectra of close-packed Au/CdSe NP mixed monolayer films. The mixing ratio (Au:CdSe) of the samples is 0:100, 4:96, 38:62, and 100:0, respectively. (b) Normalized peak intensities are shown as a function of the Au NP fraction. The broken line shows the ratio of the CdSe NPs in the film. The Inset: PL spectra measured under cw-excitation at 3.06 eV with varying Au NP fraction, x .

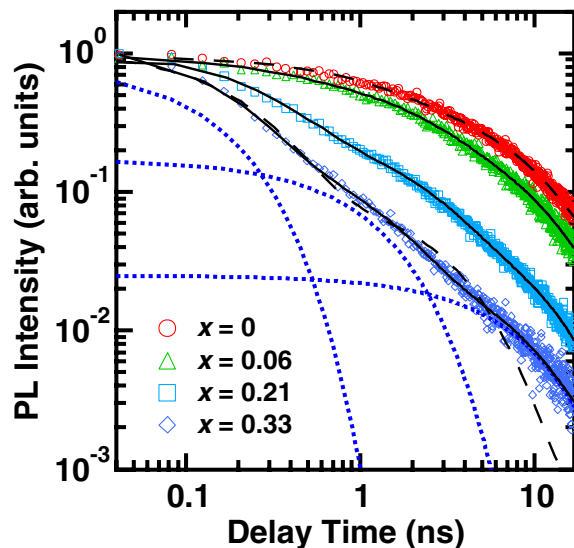


FIG. 3 (color online). PL decay dynamics of close-packed Au/CdSe NP mixed monolayer films under band-to-band excitation at 3.1 eV. The decay curves are normalized at a delay time of zero. Fitting results using two (broken line) and three (solid lines) exponential decays. The dotted lines show the three decay components in the $x = 0.33$ film.

decay component is due to the energy transfer between the CdSe NPs.

Furthermore, in the CdSe and Au NP mixed monolayer samples, rapid PL decay occurred as the Au NP ratio increased. In the mixed monolayer samples, the PL decay curves can be reproduced successfully using three exponential decay components: $I_{\text{PL}}(t) = \sum_{i=1,2,3} I_i \exp(-\frac{t}{\tau_i})$, where τ_i^{-1} are the decay rates and I_i are the amplitude. Typical examples of the fitting results are shown by the solid lines in Fig. 3. The dotted lines indicate the three decay components in the $x = 0.33$ film. For comparison, the best fitting results using the two exponential decays is shown by a broken line in the $x = 0.33$ film: the data in the nanosecond time region cannot be well reproduced by two exponential decays. These results indicate that three kinds of decay channel of excited states exist in the close-packed CdSe/Au NP monolayer.

Figure 4(a) summarizes the obtained decay times (τ_i , $i = 1, 2, 3$) as a function of the Au NP mixing ratio. The decay times are classified into three components: $\tau_1 \sim 0.2$ ns, $\tau_2 \sim 1$ ns, and $\tau_3 \sim 10$ ns. These decay times are almost independent of the Au NP mixing ratio in the film. The largest decay time, τ_3 , is roughly equal to the exciton lifetime in isolated CdSe NPs in solution, and this originates from radiative recombination within CdSe NPs in the films. As the Au NP fraction increases, the amplitudes of two slower components ($\tau_2 \sim 1$ ns and $\tau_3 \sim 10$ ns) decrease and the amplitude of the fast decay component ($\tau_1 \sim 0.2$ ns) becomes dominant. These results indicate that the fast PL quenching is caused by the energy transfer to Au NPs for the CdSe NPs in contact with Au NPs. This

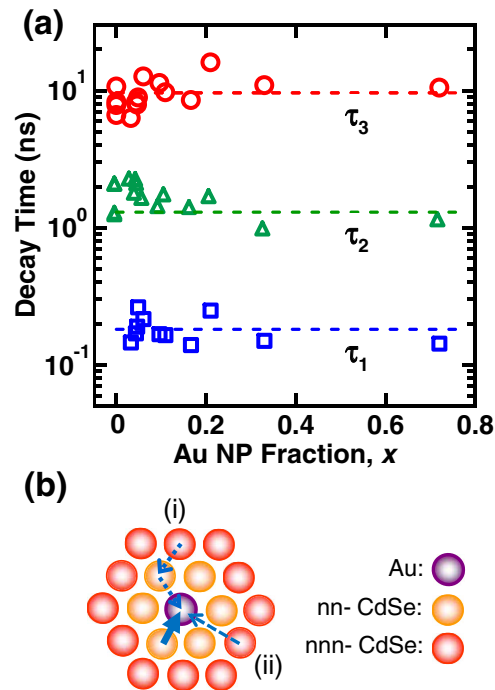


FIG. 4 (color online). (a) Decay time obtained by fitting using the three exponential decays as a function of the Au NP fraction. The broken lines are guides. (b) Schematic illustration of the configurations of the metal and semiconductor NPs. Direct energy transfer from a nearest-neighbor (nn) CdSe NP (solid arrow) and from a next-nearest-neighbor (nnn) CdSe NP [broken arrow (ii)]. Stepwise CdSe \rightarrow CdSe \rightarrow Au NP energy transfer [dotted arrow (i)].

assignment is reasonable based on a theoretical model calculation, as discussed below.

The energy transfer rate from an exciton in a semiconductor NP to a plasmon in a metal NP is derived analytically under the dipole approximation [22]:

$$\gamma_{\text{non-rad, metal}}(\omega_{\text{PL}}) = \frac{3b_{\alpha}R_{\text{MNP}}^3c^3}{2d^6\epsilon_b^{5/2}\tau_{\text{rad}}\omega_{\text{PL}}^3} \text{Im} \left[\frac{\epsilon_{\gamma}(\omega_{\text{PL}}) - \epsilon_b}{\epsilon_{\gamma}(\omega_{\text{PL}}) + 2\epsilon_b} \right], \quad (1)$$

where b_{α} , d , R_{MNP} , τ_{rad} , ϵ_b , ϵ_{γ} , and ω_{PL} are the geometrical factor, distance between the Au and CdSe NP, radius of metal NP, radiative decay time, background dielectric constant, dielectric constant of metal, and PL frequency, respectively. Equation (1) provides the lower limits of the energy transfer rate because the dipole approximation is valid for the condition $d \gg R$ (NP radius) [23]. The average interparticle distance between the metal and semiconductor NP is estimated to be $d \sim 8$ nm from the TEM image, which gives a decay time of < 0.4 ns. Here, the parameters $b_{\alpha} = 2$, $R_{\text{MNP}} = 4$ nm, $\tau_{\text{rad}} = 12$ ns, $\epsilon_b = 2$, and $\epsilon_{\gamma}(2.0 \text{ eV}) = -9.33 + 1.19i$ are used. The obtained calculation agrees with the experimental results. Therefore, we conclude that the fast PL decay component τ_1 is determined by the direct energy transfer from excitons

in CdSe NPs to plasmons in Au NPs, which causes the rapid PL quenching in mixed films. This conclusion is supported by the other experimental report that the lifetime of CdSe NPs on Au flat substrate is less than 0.2 ns [16].

Here, note that the decay component τ_2 of about 1 ns is a unique characteristic of close-packed mixed NPs solids. The 1-ns decay component is also observed in the CdSe NPs monolayer, as mentioned above. Therefore, we believe that energy transfer between the nearest-neighbor CdSe NPs takes part in the slow PL quenching process of 1 ns in the mixed film. The possible candidates for the 1-ns PL quenching process are (i) the stepwise energy transfer from a CdSe NP to a CdSe NP to a Au NP and (ii) the direct energy transfer from a CdSe NP to the next-nearest-neighbor Au NP, as illustrated in Fig. 4(b). For the close-packed hexagonal solids shown in the TEM images (Fig. 1), the average distance between the CdSe NPs and the next-nearest-neighbor Au NPs is estimated to be $d \sim 14$ nm. Using this distance and Eq. (1), the estimated energy transfer rate for process (ii) is about 12 ns, which exceeds the CdSe \rightarrow CdSe energy transfer. Therefore, we assigned the 1-ns decay component to energy transfer process (i). Since the time constant of the energy transfer between CdSe NPs, $\tau_2 (\sim 1$ ns), is much larger than that between the nearest-neighbor CdSe and Au NPs, $\tau_1 (\sim 0.2$ ns), the stepwise energy transfer CdSe \rightarrow CdSe \rightarrow Au NPs is determined by the CdSe \rightarrow CdSe energy transfer and causes the PL quenching due to the energy transfer from CdSe to Au NPs on the 1-ns time-scale. Therefore, we conclude that the PL dynamics are explained by three kinds of decay channel: nearest-neighbor CdSe \rightarrow Au NP energy transfer, stepwise CdSe \rightarrow CdSe \rightarrow Au NPs energy transfer, and radiative recombination in CdSe NPs. The PL quenching of CdSe NPs occurs through rapid energy transfer from excitons in CdSe NPs to plasmons in Au NPs.

In conclusion, we reported the energy transfer dynamics in close-packed monolayer films composed of CdSe and Au NPs. Time-resolved PL measurements revealed two types of energy transfer channel from CdSe to Au NPs in mixed monolayers. The PL quenching dynamics are determined by the nearest-neighbor CdSe \rightarrow Au NPs energy transfer and the stepwise CdSe \rightarrow CdSe \rightarrow Au NPs energy transfer in close-packed films. Our observations show that close-packed mixed solids composed of NPs with different characteristics provide detailed information on the energy transfer mechanism on a nanoscale.

The authors thank Professor T. Teranishi, Dr. M. Kanehara, and Dr. H. Koike for providing the Au NP samples and Mr. T. Matsuura and Dr. H. Inouye for his kind experimental help at an early stage of the study. Part of this study was supported by a Grant-in-Aid for Scientific Research from the Japan Society for the Promotion of Science and Global Center of Excellence (G-COE) pro-

gram from the Ministry of Education, Culture, Sports, Science and Technology of Japan.

*Corresponding author.

kanemitsu@scl.kyoto-u.ac.jp

- [1] L. Brus, J. Chem. Phys. **90**, 2555 (1986).
- [2] Y. Kanemitsu, Phys. Rep. **263**, 1 (1995).
- [3] A. P. Alivisatos, J. Phys. Chem. **100**, 13 226 (1996).
- [4] S. A. Empedocles, R. Neuhauser, K. Shimizu, and M. G. Bawendi, Adv. Mater. **11**, 1243 (1999).
- [5] E. C. Scher, L. Manna, and P. Alivisatos, Phil. Trans. R. Soc. A **361**, 241 (2003).
- [6] V. I. Klimov, J. Phys. Chem. B **110**, 16 827 (2006).
- [7] C. B. Murray, C. R. Kagan, and M. G. Bawendi, Science **270**, 1335 (1995).
- [8] M. P. Pileni, J. Phys. Chem. B **105**, 3358 (2001).
- [9] D. M. Adams, L. Brus, C. E. D. Chidsey, St. Creager, C. Creutz, C. R. Kagan, P. V. Kamat, M. Lieberman, S. Lindsay, R. A. Marcus, R. M. Metzger, M. E. Michel-Beyerle, J. R. Miller, M. D. Newton, D. R. Rolison, O. Sankey, K. S. Schanze, J. Yardley, and X. Zhu, J. Phys. Chem. B **107**, 6668 (2003).
- [10] C. R. Kagan, C. B. Murray, M. Nirmal, and M. G. Bawendi, Phys. Rev. Lett. **76**, 1517 (1996); C. R. Kagan, C. B. Murray, and M. G. Bawendi, Phys. Rev. B **54**, 8633 (1996).
- [11] S. A. Crooker, J. A. Hollingsworth, S. Tretiak, and V. I. Klimov, Phys. Rev. Lett. **89**, 186802 (2002).
- [12] M. Achermann, M. A. Petruska, S. A. Crooker, and V. I. Klimov, J. Phys. Chem. B **107**, 13 782 (2003).
- [13] O. I. Mićić, K. M. Jones, A. Cahill, and A. J. Nozik, J. Phys. Chem. B **102**, 9791 (1998).
- [14] V. I. Klimov, A. A. Mikhailovsky, Su Xu, A. Malko, J. A. Hollingsworth, C. A. Leatherdale, H.-J. Eisler, and M. G. Bawendi, Science **290**, 314 (2000).
- [15] K. T. Shimizu, W. K. Woo, B. R. Fisher, H. J. Eisler, and M. G. Bawendi, Phys. Rev. Lett. **89**, 117401 (2002).
- [16] Y. Ito, K. Matsuda, and Y. Kanemitsu, Phys. Rev. B **75**, 033309 (2007).
- [17] Z. Gueroui and A. Libchaber, Phys. Rev. Lett. **93**, 166108 (2004).
- [18] J. S. Biteen, D. Pacifici, N. S. Lewis, and H. A. Atwater, Nano Lett. **5**, 1768 (2005).
- [19] T. Shimizu, T. Teranishi, S. Hasegawa, and M. Miyake, J. Phys. Chem. B **107**, 2719 (2003).
- [20] A. Taleb, C. Petit, and M. P. Pileni, J. Phys. Chem. B **102**, 2214 (1998).
- [21] G. Nair and M. G. Bawendi, Phys. Rev. B **76**, 081304(R) (2007).
- [22] A. O. Govorov, G. W. Vryant, W. Zhang, T. Skeini, J. Lee, N. A. Kotov, J. M. Slocik, and R. R. Naik, Nano Lett. **6**, 984 (2006).
- [23] The theoretically calculated energy transfer rate is based on the dipole approximation and provides a rough estimation. More sophisticated model calculations are necessary for detailed quantitative discussions.